This is a post-peer-review, pre-copyedit version of an article published in 'Analytical and Bioanalytical Chemistry'. The final authenticated version is available online at: https://doi.org/10.1007/s00216-006-0333-5
https://pubs.rsc.org/en/content/articlehtml/2014/cp/c4cp02379j

# Competing reactions of selected atmosphericgases on $Fe_3O_4$ nanoparticles surfaces

N. Eltouny and Parisa A. Ariya

Heterogeneous reactions on atmospheric aerosol surfaces are increasingly considered importantin understanding aerosol–cloud nucleation and climate change. To understand potential reactions in polluted atmospheres, the co-adsorption of $NO_2$ and toluene to magnetite ($Fe_3O_4$ *i.e.* $FeO{\cdot}Fe_2O_3$) nanoparticles at ambient conditions was investigated for the first time. The surface area, size distribution,and morphology of $Fe_3O_4$ nanoparticles were characterized by BET method and high-resolution transmission electron microscopy. Adsorption isotherms, collected by gas chromatography with flame ionization detection, showed that the presence of $NO_2$ decreased the adsorption of toluene. The analyses of the surface chemical composition of $Fe_3O_4$ by X-ray photoelectron spectroscopy (XPS) reveal that, upon the addition of $NO_2$, the surface is oxidized and a contribution at 532.5 0.4 eV in theO1s spectrum appears, showing that $NO_2$ likely competes with toluene by dissociating on $Fe^{2+}$ sites andforming $NO_3^-$. Different competing effects were observed for oxidized $Fe_3O_4$; oxidation occurred when exposed solely to $NO_2$, whereas, the mixture of toluene and $NO_2$ resulted in a reduction of the surface *i.e.* increased $Fe^{2+}/Fe^{3+}$. Analyses by time of flight secondary ion mass spectrometry further suggest toluene reacts with $Fe^{3+}$ sites forming oxygenated organics. Our results indicate that on reduced magnetite, $NO_2$ is more reactive and competes with toluene; in contrast, on oxidized $Fe_3O_4$, toluene is more reactive. Because magnetite can assume a range of oxidation ratios in the environment, different competing interactions between pollutants like $NO_2$ and toluene could influence atmospheric processes, namely, the formation of $Fe^{2+}$ and the formation of atmospheric oxidants.

## Introduction

Heterogeneous reactions between trace gases on aerosol particlescan strongly affect the chemical and physical properties of the atmosphere.[1,2]

Iron oxides are important components of aerosol dust particlesthat can interact with trace gases such as $NO_2$, $H_2O$, and organiccompounds.[3,4] The nature of the interaction depends on the properties of the gas and the surface active sites. For example, the first step in the heterogeneous oxidation of $NO_2$ into $NO_3$ ona-$Fe_2O_3$ occurs on the iron site, where $NO_2$ is reduced to adsorbed$NO_{2(ads)}^-$.[5] In contrast, oxidation of $SO_2$ to $SO_4$ on a-$Fe_2O_3$ is suggested to begin on oxygen sites.[6] In the case of aromatic compounds, the interaction depends on the acid–base propertiesof the surface.[7] For instance, a-$Fe_2O_3$ can dehydrogenate ethyl- benzene (EB) due to the weak interaction between hard $Fe^{3+}$ acidsites and the soft basic aromatic ring of EB, whereas, softer $Fe^{2+}$acidic sites in $Fe_3O_4$ were inactive due to the stronger adsorptionwith the soft basic aromatic ring.[8] Other sites for interaction include surface defects such as oxygen and cation[9] vacancies. Namely, oxygen vacancies have been proposed to cause a catalyticcycle involving the formation of positive holes, which can oxidize$SO_2$.[10] The presence of various active sites including iron and oxygen atoms and defect sites give iron oxides adsorptive and redox properties that can alter the physical and chemical properties of the oxide surface and those of the interacting gas.

In atmospheric particles, different types of iron oxides exist andare characterized by crystal structure, which determines other properties such as conductivity and redox behavior.[11] Therefore,different phases of iron oxides are likely to display different mechanisms of interaction. For instance, in the presence of $NO_2$, cation vacancies are suggested to stabilize the formation of nitrosonium in g-$Fe_2O_3$, but not on a-$Fe_2O_3$, where vacancies are absent, resulting in different coordinating environments.[9] Investigations on the reactivity of iron oxides as components ofaerosols have been carried out mainly on a- and g-$Fe_2O_3$,[12,13] andg-FeOOH phases,[10] which serve as proxies for the iron oxide components in mineral dust, estimated to be the largest contributor to global aerosol mass.[14] In urban and industrial environments;however, aerosol particles originate from industrial[11] and traffic emissions,[15] and are composed of different phases of iron oxide:magnetite ($Fe_3O_4$ *i.e.* $FeO{\cdot}Fe_2O_3$) and, its completely oxidized form,maghemite (g-$Fe_2O_3$).[15]

Magnetite is a mixed valence iron oxide containing $Fe^{2+}$and $Fe^{3+}$, where the arrangement of $Fe^{2+}$ and half of $Fe^{3+}$ in octahedral sites allows electron hopping giving magnetite near metallic conductivity and unique redox properties.[16] Magnetite hasfound numerous catalytic applications due to its redox properties.[17] For example at temperatures in the range of 350–600 1C, magnetitecatalyzes the dissociation of water and the formation of $H_2$ gas.[18] Inthe environment, the adsorptive and redox reactivity of magnetitewith contaminants in aqueous and soil systems are known. For example, $Fe_3O_4$ adsorbs

metals by electrostatic interactions[19] (*e.g.*,Pb(II),[20] Cu(II), Zn(II), Mn(II)[19]), and reduces Hg(II) to Hg(0),[21] nitrobenzene to aniline,[22] and Cr(VI) to Cr(III).[23] In the atmosphere, anthropogenic activities involving the burning of fossil fuels emit polluting gases such as polyaromatic hydrocarbons (PAHs),[24] BTEX,[25] and NO [26] alongside dust that contains magnetite.[15]A recent field study suggested that the detection of PAHs indust collected at an industrial area is possibly due to adsorptionon magnetite present in the dust.[27]

Because of rising emissions of anthropogenic dust and gases, particularly in the vicinity of industrial regions,[28,29] the interaction between $Fe_3O_4$, as an environmental surface, and polluting gases needs to be investigated. In a previous study, weobserved that magnetite nanoparticles adsorbed gaseous benzene,toluene, ethylbenzene, and xylene (BTEX) at ambient conditions;[30]the effect of co-pollutants such as $NO_2$, was not tested, and is thesubject of this work. We report the competitive interaction of $NO_2$ and toluene on $Fe_3O_4$ nanoparticles (NPs) at room temperature (22 2 1C) and atmospheric pressure (760 5 Torr) using gas chromatography with flame ionization detection (GC-FID) to quantify the adsorption of toluene, and X-ray photoelectron spectroscopy (XPS) and time of flight secondary ion emission mass spectrometry (TOF SIMS) to analyze the chemical composi-tion of the surface. We will discuss the implications of our results on air quality and climate.

# Experimental

## Synthetic procedure

$Fe_3O_4$ NPs synthesis. The synthesis of $Fe_3O_4$ NPs was based on the procedure reported by Vereda *et al.*,[31] where a 2 : 1 mixture of solid $FeCl_3{\cdot}6H_2O$ (498%, Sigma Aldrich) and $FeCl_2{\cdot}4H_2O$ (Z99%, Sigma Aldrich) is dissolved in de-oxygenated water at 85 1C andthen co-precipitated by $NH_3{\cdot}H_2O$ (Z25% $NH_3$, Fisher Scientific). The NPs were rinsed with de-oxygenated water to remove $NH_4Cl$by-products.‡ The rinsed NPs were dried in a vacuum oven at50 1C and stored in a vacuum desiccator. Water was obtained from a Milli Q (18.2 MO cm at 25 1C, Simplicity 185). The initial oxidation ratio of the NPs was controlled by the number of washings with water, *i.e.*, the higher the number of washings, the more oxidized the $Fe_3O_4$ NPs. To characterize potential maghemite formation, X-ray diffraction (XRD) patterns show the bulk of nanoparticles was made of magnetite. With respectto XPS spectral fitting, applying constraints that correspond to maghemite alone and other phases of iron oxides (*e.g.*, FeO), did not reproduce the experimental data. Moreover, the solid synthesized powder was black, which points to magnetite. Note that considering that the NPs are 5–20 nm in size with an average size of 9 nm and that the escape depth of XPS is in that same order of a few nm (1–10 nm),[32] the spectra obtained are reflective of the whole particle and not just the surface. On thatbasis and considering that the experiments were carried out in dry air and at room temperature, any oxidation is expected to berelated to $Fe^{2+}$ from magnetite resulting in maghemite, themost favorable oxidation product. In addition, the uptake of Fe(II) as a sorbed species to magnetite in aqueous media has been shown to be unlikely and that a partially oxidized magnetitephase was more likely to form.[22]

## Characterization methods

The $Fe_3O_4$ NPs were characterized using several techniques. The crystal structure and the average Scherrer size were determined from X-ray diffraction (XRD) patterns. Details on the collection ofXRD patterns are given in Table S1 (ESI†). The morphology and size distribution of the $Fe_3O_4$ NPs were determined from images collected by means of transmission electron microscopy (PhilipsCM200 TEM). The Brunauer–Emmett–Teller (BET) specific surfacearea (SSA) and the Barrett–Joyner–Halenda (BJH) average pore sizewere determined using a surface area analyzer at –196 1C (TriStar 3000 V6.07 A). The TEM, SSA, and BJH pore size resultsare representative of a typical batch of $Fe_3O_4$ NPs prepared by co-precipitation of iron salts.

## Adsorption and surface analyses by XPS and TOF SIMS experiments

Adsorption isotherm reactions. The adsorption experiments were reproduced several times on different batches of NPs; here, we present one set of adsorption isotherms from a typicaladsorption reaction carried out on two fractions from a batch labeled $S_{adsorption}$. One of the principal objectives of this study was to investigate the system at conditions relevant to the environment. To this end, solid-phase micro-extraction (SPME) by means of a Carboxen/poly(dimethylsiloxane) (CAR/PDMS) fibre (Sigma Aldrich) was used to pre-concentrate and detect low ppmv levels of toluene. The CAR/PDMS SPME fibre consistsof a fused silica fibre coated with PDMS in which porous carbon particles are embedded rendering it suitable for the samplingof volatile organic compounds.[33] Using SPME, the lower rangeconcentrations were well reproduced. At higher concentrationsof analyte, however, SPME is not well

adapted[34] and large uncertainties result. Therefore, the majority of the isotherm data points were collected in the low concentration range of toluene.

Surface analyses by XPS and TOF SIMS. For the analyses by XPS, three fractions from each of two batches of $Fe_3O_4$ NPs, $S_{reduced}$ and $S_{oxidized}$, were subjected to different experimental conditions. For the analyses by TOF SIMS, four additional fractions from the $S_{oxidized}$ were tested. All experiments were carried out at room temperature (22 2 1C) and atmospheric pressure (760 5 Torr). As the NPs were in powdered form andmagnetic, after weighing, a magnetic stirring bar coated with Teflon was used to collect the powder. Both the magnetic bar and the powder were transferred to glass flasks, sealed with Teflon caps and stoppers. The adsorption isotherms were collected over a period of 7–8 hours. We had previously observed that the adsorption occurred on a time scale of severalminutes and determined the time for diffusion of toluene as15 minutes. The duration between two points of the isotherm is approximately 40 minutes, since several experimental conditionswere tested simultaneously in different flasks to assure data quality. As such, we performed control tests containing toluene only and serving to construct the calibration curve, the referenceand the targeted experiment. With respect to TOF SIMS and XPSexperiments, the NPs were exposed to the respective gas mixturesfor *ca.*, 18 hours prior to analysis.

All the flasks were Pyrex glass, pre-coated with a hydrophobic layer of Glassclad 18 (United Chemical Technologies[35]). Prior to adsorption experiments, the flasks were washed using hydro- chloric acid, followed by rinsing with water; subsequently withglassware soap and then with at least two portions of 20 mL ofacetone. The glass flasks were placed in an air ventilated oven at120 1C for a minimum of 12 hours. All openings were sealed with Teflon stoppers, which were also rinsed with soapy water and dried by pure airflow. To ensure the absence of organic residues,the preparation of each flask prior to the experiment started with the evacuation to at least $2 \times 10^{-2}$ Torr for 20 minutes using a Schlenk vacuum system. Then the flasks were filled with UHP $N_2$ to 760 5 Torr and re-evacuated to low $10^{-2}$–$10^{-3}$ Torr. This cycle was repeated once more, and after the second evacuation, the flask was filled by extra dry air ($O_2$ 19.5–23.5% and $H_2O$ o 10 ppm,Praxair Canada, Inc.) to 760 5 Torr. The flasks were then placedon stirring plates and allowed to stir for at least 15 minutes andthen sampled and analyzed using SPME and GC-FID (HP 6890)

equipped with a general purpose column (HP5 MS, Agilent). A peak assigned to toluene was sometimes detected, in which case theflask was subjected to further cleaning. The flasks were also analyzed by GC-MS (HP 5973, Agilent) and an HP5 MS column inscan mode verified that organic residues were not present. Thechromatogram of a typical flask prior to the addition of toluene and$NO_2$ is shown in Fig. S1 in the ESI.† Therefore, it is not likely that organic residues were left on the walls of the flasks in quantitiessufficient to impact the reaction.

Preparation of gas mixtures. For the mixture of toluene (99.8%, Fisher Scientific), liquid toluene was injected intothe flask and two pump–freeze–thaw purification cycles were carried out. After the second thaw, the pressure of toluene wasmeasured at room temperature (22 2 1C). $NO_2$ was directly transferred from a premixed 1.02% $NO_2$ in $N_2$ (Praxair Canada,Inc.) mixture into another flask. Ultrahigh purity (UHP) $N_2$ (99.999%, MEGS Specialty Gases) was used to complete toluene and $NO_2$ mixtures to 760 5 Torr. Toluene and/or $NO_2$ were injected in the reaction flasks with gas tight syringes (HamiltonCompany Inc.).

Adsorption reactions. By injecting increments of toluene into three reaction flasks, a control, a reference, and a test, adsorption isotherms of toluene on $Fe_3O_4$ NPs, in the presence and absence of $NO_2$, were collected. Prior to toluene and $NO_2$ injections, the flasks containing the $Fe_3O_4$ NPs were evacuatedfor 20 minutes (down to $6 \times 10^{-2}$ Torr), flushed with UHP $N_2$, and then filled with extra dry air. Experimental conditions are summarized in Table 1.

The amount of toluene adsorbed was determined using a CAR/PDMS SPME fibre for sampling and a GC-FID (HP 6890) for quantification. Details on data acquisition are given in the ESI.†

A calibration curve relating the FID's response (peak areas)to the range of concentrations tested was constructed using thecontrol flask, and was used to determine the amount of tolueneat equilibrium in the reference or test flasks. The amount of adsorbed toluene was calculated by subtracting the amount at equilibrium (in the reference or test flasks) from that in the control. We plotted the amount of toluene adsorbed per gram of $Fe_3O_4$ NPs as a function of the concentration of toluene remaining in the gas phase, and used adsorption models to reproduce the data. Origin Pro.8 software was used for linear and nonlinear regression of the calibration curve and adsorption isotherms, respectively.

Surface analyses with XPS and TOF SIMS. Identical prepara- tion procedures as those for adsorption reactions were followedfor each fraction of each batch with the exception of the concentration tested and the weight of NPs used. Table 1 shows theexperimental conditions. High resolution XPS scans of the carbonC1s, oxygen O1s, iron Fe2p, and N1s core lines of $Fe_3O_4$ NPs werecollected by means of an XPS unit (ESCALAB 3 MKII de VG) with anon-monochromatic Al Ka source

operated at pass energy of 20 eVand step size of 0.05 eV at a resolution of 0.85 eV. All bindingenergies reported in this work are within 0.4 eV. The spectral analyses of the scans were carried out using the Avantage software[36] (Thermo Scientific). Details on the spectral fitting, peak assign- ments for Fe2p, and C1s spectra are presented in Fig. S2 and S3 and Table S2 (ESI†). TOF SIMS mass to charge spectra of $Fe_3O_4$ NPswere obtained for positive and negative ions on a unit (ION-TOFSIMS IV) with a $Bi^+$ ion source at 25 kV.

Table 1 Experimental conditions for adsorption and surface analyses

| | Toluene (ppmv) | $NO_2$ (ppmv) | $Fe_3O_4$ NPs (g) ± $2.0 \times 10^{-4}$ |
|---|---|---|---|
| Adsorption | | | $S_{adsorption}$ |
| Control | 0–1200 | 1.5 | — |
| Reference | 0–1200 | | 0.14 |
| Test | 0–1200 | 1.5 | 0.14 |
| XPS | | | $S_{reduced}$ |
| (a) | — | — | 0.02 |
| (b) | 13 | — | 0.02 |
| (c) | 13 | 0.65 | 0.02 |
| XPS and TOF SIMS | | | $S_{oxidized}$ |
| (a) | — | — | 0.02 |
| (b) | 13 | — | 0.02 |
| (c) | 13 | 0.65 | 0.02 |

## Results and discussion

Characterization of the $Fe_3O_4$ NPs

The XRD patterns of $Fe_3O_4$ NPs in Fig. 1 show that relative intensity peaks for $S_{adsorption}$, $S_{reduced}$, and $S_{oxidized}$ matched those of the reference $Fe_3O_4$, for which the Scherrer size was calculated as 8 and 9 nm,[37] respectively.

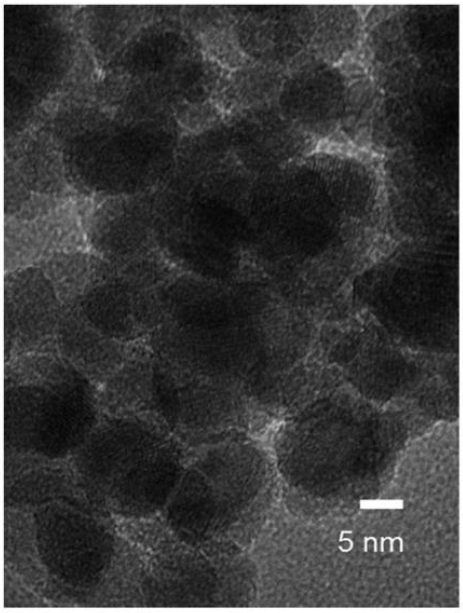


Fig. 2 A typical high resolution TEM image depicting the size distribution and crystallinity of $Fe_3O_4$ NPs prepared by co-precipitation.

For a typical $Fe_3O_4$ prepared by co-precipitation, the SSA was 80 10 $m^2$ $g^{-1}$ and the average pore width was 10 3 nm varyingfrom 5–50 nm,[30] which indicates NPs were mesoporous.[38] The TEM image in Fig. 2 shows the size distribution of the $Fe_3O_4$ NPswas in the range of 5–10 nm and the NPs were crystalline. The sizerange and pore widths of the NPs indicate they were geometricallyheterogeneous.

Adsorption reactions

Competitive adsorption of toluene and $NO_2$ on $Fe_3O_4$ NPs. To investigate the effects of $NO_2$ on the adsorption of toluene on $Fe_3O_4$ NPs, adsorption isotherms of toluene, alone and in the presence of 1.5 parts-per-million by volume (ppmv) $NO_2$, were collected. The adsorption experiments were carried out several times and the trend of a decrease in the adsorption of toluene in the presence of $NO_2$ is reproduced for seven independentexperiments, but to different extents. The variability in the adsorption capacity of toluene to the NPs was observed and ranged from 10 to 40% across different batches of NPs. A batchcorresponds to a single separate synthesis of NPs.

This variability is attributed to the variability existing acrossdifferent batches of the NPs. The variability between batches ofNPs is likely related to different initial oxidation levels of the different batches used and the size distribution and morphology.The latter would affect the surface area available, while the former would influence specific sites for adsorption ($Fe^{2+}$ and $Fe^{3+}$) and properties such as acid–base character. The oxidationlevel of a batch of NPs could have been affected by the time required for drying and the storage time from synthesis to use. The highest vacuum during drying and storage was 18 Torr, which means that the NPs could have been exposed to air. Magnetite is sensitive to oxygen in air and a layer of oxidized magnetite (*i.e.* maghemite g-$Fe_2O_3$) is known to form on the surface,[39] resulting in different initial oxidation levels. With respect to the variability in size and morphology, the synthesisof NPs by co-precipitation results in polydispersed samples dueto the mechanism of formation (during nucleation and growth stages).[40] Inhomogeneity of the sizes of the NPs could affect theavailable sites for adsorption and result in the variability with respect to the extent of adsorption. Prior to adsorption and characterization experiments, the NPs were crushed with amortar and pestle, which results in variability in size as observedin the TEM image (Fig. 2). For each set of experiments comprisedof toluene and toluene + $NO_2$, fractions of NPs came from the same batch. Examples of other adsorption experiments are givenin the ESI† (Fig. S4 and S5). A typical adsorption

experiment isshown in Fig. 3, where the adsorption of toluene on $Fe_3O_4$ NPs is reduced in the presence of $NO_2$. The reduction in the adsorptionof toluene on a related oxide, $Fe_2O_3$ in the presence of $NO_2$ hasbeen observed (at 117 1C).[41] The reduction in the amount of toluene adsorbed indicates that $NO_2$ competes with toluene in the same sites.

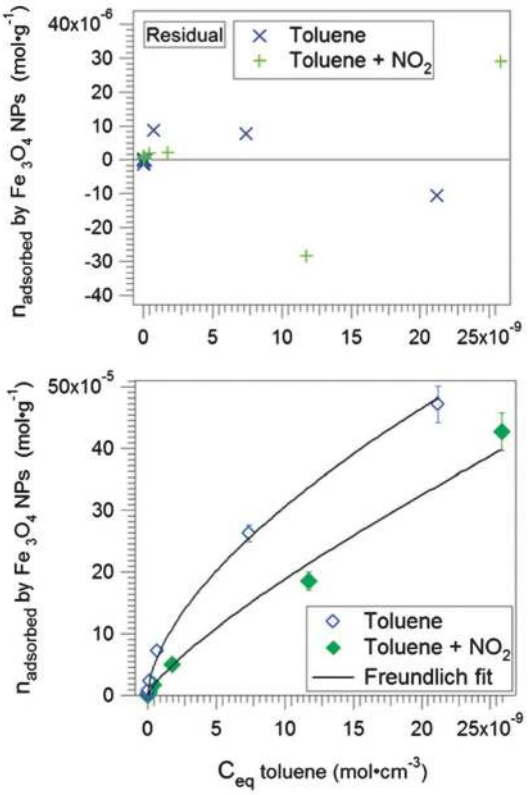


Fig. 3 Experimental and fitted adsorption isotherms (bottom graph) and residual of the fit (top graph) of toluene on $Fe_3O_4$ NPs in dry air alone (blue empty diamonds) and in the presence of $NO_2$ (green filled diamonds). Error bars represent standard errors calculated by the propagation of errors during preparation and analyses. The limit of detection of toluene is $(3.3 \times 10^{-13}) \pm (3.1 \times 10^{-15})$ mol $cm^{-3}$. 1 ppmv of toluene = $4.11 \times 10^{-11}$ mol $cm^{-3}$.

To further examine the mechanism by which $NO_2$ reduces the adsorption of toluene, several adsorption models frequentlyused to represent vapor–solid adsorption were attempted including Langmuir,[42] Freundlich,[43] Toth,[44] Sips,[45] Redlich– Peterson,[46] and dissociative Langmuir.[47] These models differ in the assumptions made to describe the adsorption of vapor to a surface. Table S3 (ESI†) enlists the models used, their respectiveassumptions and parameters (*e.g.*, energy of sites, interactions between adsorbed molecules *etc.*). The parameters relevant to each model were determined by nonlinear regression method based on the minimization of $w^2$. The resulting fits and residualsfor the models tested are plotted in Fig. S6 (ESI†) and the respective values for the parameters are presented in Table S4 in the ESI.† Among the tested models, RP, Toth, Sips, and Freundlich appear to reproduce the observed isotherm more adequately at the higher concentration. In both Toth and Sips test models, however, the fitting resulted in higher standard errors on the measured parameters.

To evaluate the RP and Freundlich test models, we used the comparison fitting tool in OriginPro 8S[48] based on the AIC criterion test, which ranks the models in order of most justified to represent the data and has been used in several previous adsorption/ desorption modeling studies.[49,50] Details on the calculations are presented in the ESI.† On the basis of the AIC criterion, the RP model is 0.38 times more likely to be correct. In other words, bothFreundlich and RP are similar. Since the number of data pointsmodeled was 10, we selected the model with fewer parameters (*i.e.*, Freundlich). The Freundlich model is represented by eqn (1):

$$n_{ads} = K_F C_{eq}^{\frac{1}{n}} \quad (1)$$

where the constants $K_F$ and $n$ represent the Freundlich constants.The residuals are shown in the top graph in Fig. 3.

The parameter values for the Freundlich model are shownin Table 2. The Freundlich model describes adsorption onenergetically heterogeneous sites.[51] The constants, $K_F$ and $n$, are specific to the adsorption system and depend on temperature.Together, $K_F$ and $n$ provide a measure of adsorption capacity thatdepends on the heterogeneity[52] in the system due to lateral interaction and surface sites (geometric and chemical), which areencompassed in '$n$'.[53] Therefore, the use of the Freundlich modelsuggests that the adsorption mechanism of toluene occurs on heterogeneous sites, which could be explained by the range of sizes and pore widths of NPs (Fig. 2), but also by the presence of $Fe^{2+}$ and $Fe^{3+}$ as chemically heterogeneous sites. The Freundlichisotherm has been reported to model toluene vapor on heterogeneous surfaces like soil,[54] and carbon nanotubes,[55] and the adsorption of heavy metals from aqueous media on $Fe_3O_4$,[20] and on $\gamma$-$Fe_2O_3$.[56]

In the presence of $NO_2$, despite showing the best fit for the data, a large standard error in the $K_F$ value suggests the model may be oversimplifying the interaction of toluene. Nevertheless, if we compare the '$n$' values, the system involving $NO_2$ has a lower value. Because '$n$' is sensitive to the composition of the adsorption system,[52] a lower '$n$' implies that $NO_2$ influences the adsorption of toluene by decreasing heterogeneous processes. There are several processes that can be affected by $NO_2$ such as blockingsites (*e.g.*, pores), and/or reacting with the active sites for adsorptionof toluene (*i.e.* $Fe^{2+}$ and $Fe^{3+}$). To further understand the mechanism by which $NO_2$ competes with toluene, surface analyses of the $Fe_3O_4$ were carried out by XPS and TOF SIMS and are discussed in the next section.

**Table 2** Parameter values for the Freundlich fit of the adsorption isotherms of toluene on $Fe_3O_4$ NPs in dry air alone and in the presence of $NO_2$

| Parameters | Toluene | Toluene + $NO_2$ |
|---|---|---|
| $K_F$ ($cm^{-3}$ $g^{-1}$) | $(2.01 \times 10^1) \pm 4.6$ | $(3.75 \pm 2.24) \times 10^2$ |
| $n$ | $1.66 \pm (3.2 \times 10^{-2})$ | $1.27 \pm (5.1 \times 10^{-2})$ |

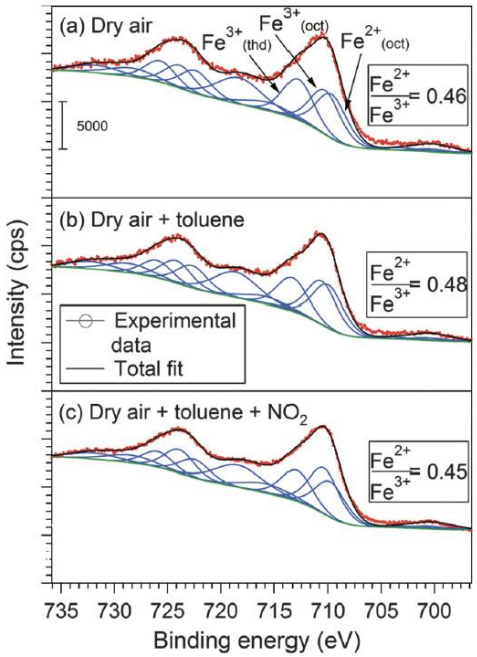


**Fig. 5** Fe2p XPS fitted spectra for fractions from $S_{reduced}$.

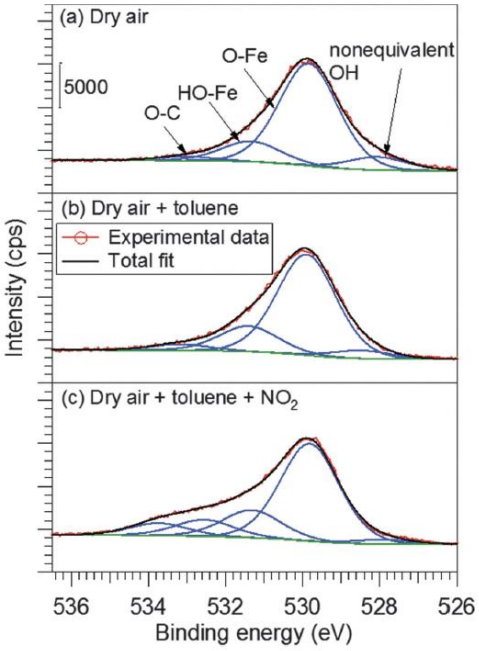


**Fig. 4** O1s XPS fitted spectra for fractions from $S_{reduced}$.

Surface analyses of the $Fe_3O_4$ NPs

XPS and TOF SIMS of samples exposed to dry air only. Toanalyze the chemical composition of the surface of $Fe_3O_4$ NPs in dry air and in the presence of toluene and/or $NO_2$, the high resolution spectra XPS of O1s and Fe2p were collected. The XPSO1s and Fe2p spectra in dry air only are shown in Fig. 4(a) and5(a), for the fraction from batch $S_{reduced}$, and Fig. 6(a) and 7(a), forthe fraction from $S_{oxidized}$. The O1s spectra in Fig. 4(a) and 6(a) arefitted with 3 peaks at 529.8 eV, 531.3 eV, and 533.0 eV, which wereassigned to the main oxide FeO, lattice FeOH and/or adsorbed hydroxyl, and (O–C) and/or adsorbed water, respectively. The peakat 533.0 0.4 eV can be assigned to water, but also to organic O(O–C).[57,58] The atomic percent contribution of the O–C in theO1s correlates with that in the C1s (S2 and S3, ESI†). Therefore,the peak is likely O–C. Since adsorbed water can also be found dueto moisture in the air, it cannot be ruled out as another potentialadsorbed species. The source of the carbon contamination is due to air exposure and possibly reactions involving $CO_2$ at vacuum levels during the XPS analysis.[59] With respect to adsorbed moisture, studies on hydrated iron films show that carbon contamination may also dissolve into the water layer and result in the contribution for O–C.[60] These values are consistentwith reported values for $Fe_3O_4$, as shown in Table 3. A contributionat 528 eV was added, and is likely a hydroxyl group. Peaks below themain oxide have been assigned to chemisorbed oxygen and hydroxylgroups at non-equivalent sites of $Fe_3O_4$ exposed to $H_2O$.[61] Note thatthe formation of strongly bound hydroxyl groups[62] on magnetiteoccurs due to the dissociation of moisture, which is reported for $H_2O$ present at pressures as low as $10^{-4}$ Torr,[61] and could form during sample preparation (*e.g.*, weighing and transferring). The Fe2p spectra in Fig. 5(a) and 7(a) show the $Fe^{2+}/Fe^{3+}$ were 0.46 and 0.38 for $S_{reduced}$ and $S_{oxidized}$, respectively. Note that stoichiometric $Fe_3O_4$ has a ratio of 0.50. The estimated randomerror on all reported $Fe^{2+}/Fe^{3+}$ ratio values are presented in Table 3; details are given in the ESI.†

Interaction of toluene with $Fe_3O_4$ NPs. Using XPS, theprimary objective was to examine changes in the surface redoxratio. In the presence of toluene, Fig. 5(a) and (b) show that $Fe^{2+}/Fe^{3+}$ increases slightly from 0.46 to 0.48, but is within experimental uncertainty. In the case of $S_{oxidized}$ exposed to 13 ppmvof toluene, contamination on the carbon spectrum was observedand the sample was excluded from the comparison. However, duringthe same set of experiments, a fraction of $S_{oxidized}$ exposed to 100 ppmv of toluene (in dry air) was tested and the $Fe^{2+}/Fe^{3+}$ increased from 0.38 to 0.49, shown in Fig. 7(a) and (b) and Table 3. We had previously observed an increase in the $Fe^{2+}/Fe^{3+}$ when exposed to toluene.[30] The increase in the $Fe^{2+}/Fe^{3+}$ ratio could result if toluene reacts on the $Fe_3O_4$. More details on the uncertainties associated with the changes in the $Fe^{2+}/Fe^{3+}$ in thepresence of toluene alone are given in the ESI.†

With respect to the XPS O1s spectra, an increase in the ratio

of organic oxygen/total O is observed for both $S_{reduced}$ and $S_{oxidized}$ samples exposed to toluene alone, as shown in Table 3. The contributions assigned to organic oxygen are consistent with organic carbon observed in the C1s. In the caseof $S_{reduced}$, there is a decrease in the Fe/O when toluene is added, which appears to be consistent with the increase in theorganic oxygen. Note that the initial Fe/O is larger than the theoretical value of 0.75. The reason for the higher content of iron is unclear. In the case of $S_{oxidized}$, the Fe/O is constant and is inconsistent with the increase in the organic O. However, theratio of organic oxygen/Fe–O (oxide) increases for both $S_{reduced}$and $S_{oxidized}$ when exposed to toluene. The increase in theorganic oxygen appears to occur at the expense of the oxide suggesting that toluene interacts with the oxygen from the oxide; yet it is noteworthy that these changes are close to the uncertainty limits, a definite mechanism cannot thus be confirmed,at this stage. In Table 4, the TOF SIMS analyses for fractions exposed to toluene show increases in the normalized intensitiesfor fragments associated with toluene at *m/z* of 77 and 91. The increase in fragments at *m/z* 43 and 105, associated with oxygenated compounds further hint that toluene is reacting. The TOF SIMS spectra showing the total intensity of the fragmentshaving *m/z* of 43, 77, 91, and 105 for the fractions of $Fe_3O_4$ NPsexposed to various conditions (Table 1) are shown in Fig. S7–S10 inthe ESI.† Note that the inherent presence of hydrocarbons as impurities in TOF SIMS analyses precludes a definite reactive mechanism which is to be ascertained. Under conditions similarto those used here, the adsorption of toluene on $Fe_3O_4$ is explained by the acid–base properties of the system, where thearomatic ring (base site) interacts with the partially filled d-shellsof the iron cations (acid site), an interaction observed for otheroxides[7] and, between cations and polyaromatic compounds in soils[63] (and references therein).

Reactions of aromatic compounds adsorbed on metal oxides

have been observed under non-ambient conditions *e.g.*, at temperatures greater than 300 1C.[64] For example, the dehydro-genation of ethylbenzene (EB) on a-$Fe_2O_3$, and the oxidation of toluene on iron based catalysts[64] were proposed to occur *via*C–H activation of the ethyl and methyl groups followed by hydrogen abstraction by basic oxygen in the oxide, which in the case of EB was proposed to cause a reduction of the nearby $Fe^{3+}$ to $Fe^{2+}$.[8,65]

Since all experiments were performed at room temperature,it is proposed that the reactivity be associated with

defects and/or nanoscale effects of $Fe_3O_4$ NPs. Step defects on a-$Fe_2O_3$ havebeen proposed to cause adsorption of EB in a particular configuration favoring H-abstraction.[66] Defects such as oxygen vacancies, known to occur in solids to maintain charge neutrality,[67] are another type of reactive sites reported for iron oxides; the adsorption of oxygen in those vacancies results in reactive oxygenspecies.[68] In an iron supported catalyst, vacancies influenced theconfiguration of the adsorbing oxygen into an angular arrangementthat enhanced CO oxidation.[68] Here, $Fe_3O_4$ NPs samples were exposed to oxygen (*ca.*, 760 Torr of dry air) prior to toluene addition, therefore, the presence of oxygen vacancies as direct active sites isunlikely as oxygen would adsorb onto them; the presence of reactive oxygen species, however, cannot be precluded.

In addition, nanoscale effects can influence reactivity due to enhanced acid–base properties.[69] On a related oxide, higher basicity of surface oxygen atoms for smaller a-$Fe_2O_3$ NPs were proposed to explain increased oxidation of $Mn^{2+}$.[70] Alternatively, the adsorption of toluene could induce charge rearrangement. The effect of water adsorbed on the surface arrangement of iron cations in magnetite has been proposed in a recent theoretical study.[71] In summary, these results point to a complex inter- action of toluene on $Fe_3O_4$ NPs, where the observed increases inthe $Fe^{2+}/Fe^{3+}$ ratio and in the contributions assigned to organic oxygen could be due to the oxidation of toluene by surface oxygen on $Fe_3O_4$ NPs and the possible formation of an oxygenated organic.

**Oxidation of $Fe_3O_4$ NPs by $NO_2$.** For the mixture of tolueneand $NO_2$, the $Fe^{2+}/Fe^{3+}$ values of $S_{reduced}$ are lower but within the error when compared with the fraction exposed to toluene shown in Fig. 5(b) and (c). By comparing the Fe/O ratios, a decrease is observed, as shown in Table 3, and is consistent with the addition of oxygen, which supports the oxidation of the surface. In contrast, the fraction from $S_{oxidized}$ in Fig. 7(c) has a higher $Fe^{2+}/Fe^{3+}$ compared with the sample in air (Fig. 7(a)), while the Fe/O remains constant suggesting that a different mode of interaction is occurring and preventing $NO_2$ from oxidizing the surface. Note that the effect of $NO_2$ alone onthe $Fe_3O_4$ NPs was beyond the scope of the study; however, a fraction of $S_{oxidized}$ exposed to $NO_2$ only, results in the highest decrease in the $Fe^{2+}/Fe^{3+}$ ratio, *i.e.* in the oxidation of $Fe_3O_4$ NPs and is shown in Table S5 in the ESI.† In summary, the results show that the addition of $NO_2$ causes an oxidation of the surface, but that its competing effects on the adsorption of toluene depend on the initial stoichiometric ratio of magnetite. For consistency, $S_{oxidized}$ exposed to 100 ppmv of toluene was not used for comparison since the other samples were exposed to only 13ppmv(see previous section).

In the atmosphere, the reactions of $NO_2$ and hydrocarbons are influenced by the presence of hydroxyl radicals, which are formed photochemically at wavelengths in the UV($O_3$<319 nm,$O_3$ formation from $NO_2$<424 nm).[72] In our experiments, however, radiation was not applied and hydroxyl radicals in the gas phase were not present. Further qualitative and quantitative analyses by GC-MS showing that $NO_2$ and toluene did not react in the gas phase are given in Fig. S1 in the ESI.† Therefore, thechanges observed are attributed to surface reactions on the $Fe_3O_4$ NPs. The interaction of $NO_2$ with metals has been proposed to occur by adsorbing to the metal site[73] and partially dissociating into $NO_3^-$ and NO *via* the formation of $NO_2^-$,[9] following equation (2)-(4) or (5) :

$$2NO_2(g) \rightarrow 2NO_2(ads) \quad (2)$$

$$2\acute{e} + 2NO_2(ads) \rightarrow 2NO_2^-(ads) \quad (3)$$

$$NO_2^-(ads) + NO_2^-(ads) \rightarrow NO_3^-(ads) + NO(g) + \acute{e} \quad (4)$$

$$NO_2^-(ads) + NO_2(g) \rightarrow NO_3^-(ads) + NO(g) \quad (5)$$

The oxidation of magnetite is proposed to be due to the reduction of $NO_2$ to $NO_2^-$ on the iron sites *i.e.* the same active sites for toluene.

**Table 3** Assignments of binding energies (in eV) and ratios calculated from high resolution fitted spectra of Fe2p and O1s XPS for fractions of $Fe_3O_4$ NPs exposed to different experimental conditions

| | $S_{reduced}$ | | | $S_{oxidized}$ | | |
|---|---|---|---|---|---|---|
| Assigned species, reported literature BE | Dry air | Toluene | $NO_2$ + toluene | Dry air | Toluene[a] | $NO_2$ + toluene |
| OH (nonequivalent): −1.6, $O^{2-}$ (undercoordinated): −1 (rel. Fe–O)[61] | 528.1 | 528.5 | 527.9 | 527.4 | 527.3 | 528.1 |
| O–Fe: 529.9 ± 0.4,[82] 530.1 ± 0.2[83] | 529.8 | 529.9 | 529.8 | 529.8 | 529.9 | 529.9 |
| HO–Fe, adsorbed O, O═C: 531.4 ± 0.2,[83] 531.6,[39] 531.3, 531.9–532.8[58] | 531.3 | 531.4 | 531.3 | 531.3 | 531.3 | 531.4 |
| $NO_3/NO_2$ (on $TiO_2$): 532.5/533[74] O–C: 532.4–533.5[58] | | | 532.6 | | | |
| $H_2O$ on $Fe_3O_4$: 532.7 ± 0.1 γ-$Fe_2O_3$: 533.3 ± 0.1[57] $H_2O$ (molecular): 534[61] | 533.0 | 533.2 | 533.7 | 533.0 | 533.0 | 533.3 |
| $Fe^{2+}/Fe^{3+}$ | 0.46 ± 2.6 × $10^{-2}$ | 0.48 ± 2.8 × $10^{-2}$ | 0.45 ± 2.8 × $10^{-2}$ | 0.38 ± 2.0 × $10^{-2}$ | 0.49 ± 2.7 × $10^{-2}$ | 0.43 ± 2.9 × $10^{-2}$ |
| Fe/O | 0.80 ± 2.7 × $10^{-2}$ | 0.74 ± 2.5 × $10^{-2}$ | 0.63 ± 1.9 × $10^{-2}$ | 0.70 ± 2.4 × $10^{-2}$ | 0.70 ± 2.3 × $10^{-2}$ | 0.71 ± 2.9 × $10^{-2}$ |
| O > 531.2 eV/O (total) | 0.030 ± 4.1 × $10^{-3}$ | 0.040 ± 5.1 × $10^{-3}$ | 0.19 ± 9.9 × $10^{-3}$ | 0.053 ± 5.2 × $10^{-3}$ | 0.065 ± 5.6 × $10^{-3}$ | 0.059 ± 6.6 × $10^{-3}$ |
| O > 531.2 eV/Fe–O (non equiv., FeOH and FeO) | 0.030 ± 4.3 × $10^{-3}$ | 0.046 ± 5.3 × $10^{-3}$ | 0.23 ± 1.3 × $10^{-2}$ | 0.056 ± 5.5 × $10^{-3}$ | 0.069 ± 6.0 × $10^{-3}$ | 0.063 ± 7.1 × $10^{-3}$ |
| FeOH (including peak at 528)/FeO | 0.33 ± 1.4 × $10^{-3}$ | 0.33 ± 1.2 × $10^{-2}$ | 0.31 ± 1.0 × $10^{-2}$ | 0.24 ± 1.4 × $10^{-2}$ | 0.23 ± 1.3 × $10^{-2}$ | 0.27 ± 1.8 × $10^{-2}$ |

[a] Toluene concentration 100 ppmv.

In addition to oxidation, changes in the oxygen O1s of $S_{reduced}$ when $NO_2$ is added (Fig. 4(c)) are observed. An increase in oxygen is observed for the organic O/O (total) ratio compared with the fraction exposed to air or toluene alone, as shown in Fig. 4(a)–(c) and Table 3 for $S_{reduced}$. A peak at 532.6 eV has only been observed on the $S_{reduced}$ sample. Peaks at binding energiesin the range of 532.5–534 eV are assigned to organic oxygen and adsorbed water, but could also be attributed to $NO_3$ and/or $NO_2$at 532.5 eV and 533 eV, respectively.[74] However, the N1s spectradid not show peaks in the $NO_2/NO_3$ region and the TOF SIMS spectra did not positively confirm *m/z* of 46 ($NO_2^-$) or 62 ($NO_3^-$),which is explained by the low concentrations of $NO_2$ used in this work (0.65 ppmv). Nevertheless, a mechanism involving the formation of $NO_3$ cannot be ruled out. By comparing with the C1s (Fig. S2, ESI†), a peak at 289 eV consistent with organic oxygen is observed. At this stage, however, we cannot confirm theidentity of the peak at 532.5 eV, which appears to be related to the addition of $NO_2$. In the case of $S_{oxidized}$ ratios involving oxygen species are within uncertainty range, as depicted in Fig. 6(c) and Table 3. An increase in the organic O/O (total) is also observed for $S_{oxidized}$ exposed to $NO_2$ alone, as shown in Table S5 in the ESI.†

Because the surface contains hydroxy groups, an additional pathway relevant for the reaction of $NO_2$ on hydroxylated surface involves the formation of nitrate and $H_2O$, which has been reported on metal oxide.[75] Alternatively, it has also been observed that the strong interaction of $NO_2$ with the metal center on the hydroxylated surface of molybdenum oxide caused the displacement of OH and its recombination into$H_2O$ rather than reacting and forming of $HNO_3$,[76] as is typicallyreported for metal oxides. It cannot be ruled out that water forms and as previously mentioned carbon contaminants may dissolve giving rise to the organic carbon contributions.

To summarize, fractions from the $S_{reduced}$, which contained OH groups at low BE and had a higher initial $Fe^{2+}/Fe^{3+}$ ratio, were more reactive towards $NO_2$ compared with the fractions from the $S_{oxidized}$ batch, where OH was absent and the $Fe^{2+}/Fe^{3+}$ratio was lower. The binding environment of OH has been shown to influence the reactivity of related iron oxyhydroxidesFeOOH.[77] Here, the exact coordinated environments of oxygenatoms on $Fe_3O_4$ cannot be extracted by XPS due to overlappingbinding energies; further studies on the coordinating environ- ment of OH on magnetite, and the respective interactions with $NO_2$ are needed to understand the associated reactivity.

These results show that the mixture of toluene and $NO_2$ interacts on the reduced and oxidized samples *via* different pathways. In the case of reduced magnetite, the observed oxidation (decrease in $Fe^{2+}/Fe^{3+}$ and increase in oxygen) and the peak at 532.5 eV suggest that $NO_2$ either competes with toluene or is involved in the oxidation of toluene. In contrast, on the oxidized sample, the mixture of toluene and $NO_2$ results in an increase in the $Fe^{2+}/Fe^{3+}$ ratio pointing to a different reaction mechanism, where toluene either competes with $NO_2$ and/or reverses oxidation by interacting with the iron sites.

The difference in the initial stoichiometric ratio suggests that $NO_2$ is more reactive on reduced $Fe_3O_4$. On g-$Fe_2O_3$ studieshave shown that the reaction of $NO_2$ forming $NO_3$ likely involves two $NO_2^-$ adsorbed (eqn (4)),[9] and depends on the concentration of adsorbed $NO_2^-$. Therefore, the presence of more $Fe^{2+}$ could result in the formation of more adsorbed$NO_2^-$, and possibly $NO_3^-$ on the reduced sample. The higher reactivity of reduced $Fe_3O_4$ compared with its more oxidized counterpart has been reported for other systems.[78,79] For instance, in the reduction of $Cr^{+6}$, where $Fe^{2+}$ donate electrons to drive the reaction, the formation of an oxidized layer of g-$Fe_2O_3$ inhibited further reaction,[80] in aqueous media. The results indicate that the stoichiometry of magnetite will deter- mine the competing effects in a reaction mixture of toluene and$NO_2$, where reduced surfaces will get oxidized and form an irreversible product, while oxidized surfaces would be less reactive towards $NO_2$ allowing toluene to interact and resultin an increase of $Fe^{2+}$.

At this stage, we cannot propose a definitive mechanism(s) on how toluene competes with $NO_2$ for adsorption onto oxidizedsamples of $Fe_3O_4$ NPs; yet it is logical to speculate that either toluene occupies $Fe^{2+}$ sites or it can displace $NO_2$ before the formation of $NO_2^-$. The formation of $NO_2^-$ has been reported asthe rate limiting step in the production of $NO_3$ on g-$Fe_2O_3$,[9] hence could be hindered by less availability of $Fe^{2+}$, which resultsin less conductivity and electron flow necessary for the formationof $NO_2^-$. The reactivity of $NO_2$ is influenced by the nature of theactive sites, which differ for iron oxides polymorphs. Namely, inaddition to iron sites, cation vacancies on g-$Fe_2O_3$ have been linked to reactive sites that cause various coordination environ-ments in comparison with a-$Fe_2O_3$.[9] Here, oxidized magnetite contains g-$Fe_2O_3$, which may allow a different formation reaction pathway in comparison with reduced $Fe_3O_4$. With respect to oxygen vacancies, known to form reactive oxygen by adsorbingoxygen,[81] and to influence the interaction of $NO_2$ with other metal oxides,[73] as with toluene, it is unlikely that they are present as direct active sites for $NO_2$ in dry air. The presenceof adsorbed reactive oxygen, however, cannot be ruled out. Reactive oxygen species have been proposed to cause an increasein positive holes that can adsorb and oxidize $SO_2$ to $SO_4$ on a-$Fe_2O_3$,[10] and to adsorb in a particular configuration that allowedsubsequent reaction with CO forming $CO_2$ on an a-$Fe_2O_3$ basedcatalyst.[68]

Here, our results suggest that $NO_2$ interacts with iron sites, yet it is possible that if reactive oxygen species are present, the coordinating environment of $NO_2$ on iron sites be affected influen-cing the formation of nitrate.[81] Future investigations should includestudying the reaction intermediates on $Fe_3O_4$ samples of varying stoichiometric ratios. Future vibrational spectroscopy studies mightbe helpful to ascertain reactive species on the surfaces.

## Conclusion

In this work, we studied for the first time the interaction of $NO_2$and toluene on $Fe_3O_4$ NPs, to investigate potential reactions onindustrial dust aerosols. The reduction in the adsorption of toluene when $NO_2$ is added indicates a competition for active sites.

The competing effect of $NO_2$ was explained by its reactivitywith magnetite, which is suggested to depend on the availabilityof $Fe^{2+}$ and possibly $OH^-$. Previous studies in aqueous systemshave established the importance of $Fe^{2+}$ (ref. 84) in the reactivityof magnetite.[85] The results presented here expand on the importance of $Fe^{2+}$ and stoichiometry of $Fe_3O_4$, as well as the possible influence of reactive oxygen species in understandinggas solid reactions. Sorbed OH groups suggest that relative humidity can further influence the reactivity of gases on dust containing $Fe_3O_4$; the effect of relative humidity has been testedand is the subject of another study.[37]

The atmospheric implications of these reactions are of particular relevance in polluted areas, where large emissionsof anthropogenic dusts containing magnetite and mixtures of gases occur. Changes in the chemical composition of the dust particles can influence subsequent interactions such as theuptake of water vapour affecting nucleation processes leading to the formation of clouds (*e.g.*, the size of the ice crystal) as well as the type and intensity of precipitation.

## Acknowledgements

We are grateful to Dr J. Lefebvre for collecting XPS and TOF SIMS spectra and for discussions on XPS interpretation, Dr D.Deeds and an anonymous reviewer for providing constructive comments and Ms Cavaliere for proofreading the manuscript. Weacknowledge the following Canadian funding agencies: NSERC, CFI, FRQNT, and Environment Canada for financial support.

## Notes and references

1 P. J. Ziemann and R. Atkinson, *Chem. Soc. Rev.*, 2012, 41,6582–6605.
2 D. M. Cwiertny, M. A. Young and V. H. Grassian, *Annu. Rev.Phys. Chem.*, 2008, 59, 27–51.
3 S. A. Styler and D. J. Donaldson, *Environ. Sci. Technol.*, 2012, 46, 8756–8763.
4 S. Carlos-Cuellar, P. Li, A. P. Christensen, B. J. Krueger, C. Burrichter and V. H. Grassian, *J. Phys. Chem. A*, 2003, 107,4250–4261.
5 G. M. Underwood, T. M. Miller and V. H. Grassian, *J. Phys.Chem. A*, 1999, 103, 6184–6190.
6 H. Fu, X. Wang, H. Wu, Y. Yin and J. Chen, *J. Phys. Chem. C*,2007, 111, 6077–6085.
7 M. Nakazawa and G. A. Somorjai, *Appl. Surf. Sci.*, 1993, 68,517–537.
8 Y. Joseph, M. Wuhn, A. Niklewski, W. Ranke, W. Weiss, C. Woll and R. Schlogl, *Phys. Chem. Chem. Phys.*, 2000, 2,5314–5319.
9 B. C. Hixson, J. W. Jordan, E. L. Wagner and H. M. Bevsek, *J. Phys. Chem. A*, 2011, 115, 13364–13369.
10 J. Baltrusaitis, D. M. Cwiertny and V. H. Grassian, *Phys. Chem. Chem. Phys.*, 2007, 9, 5542–5554.
11 R. M. Cornell and U. Schwertmann, *The iron oxides: structure,properties, reactions, occurrence, and uses*, VCH, Weinheim;New York, 2003 edn, 1996.
12 C. Liu, Q. Ma, Y. Liu, J. Ma and H. He, *Phys. Chem. Chem. Phys.*, 2012, 14, 1668–1676.
13 J. Baltrusaitis, P. M. Jayaweera and V. H. Grassian, *Phys. Chem. Chem. Phys.*, 2009, 11, 8295–8305.
14 Y. H. Lee and P. J. Adams, *Atmos. Chem. Phys.*, 2010, 10, 2129–2144.
15 M. S. Bućko, O.-P. Mattila, A. Chrobak, G. Ziółkowski, B. Johanson, J. Čuda, J. Filip, R. Zbořil, L. J. Pesonen and

M. Leppäranta, *Geophys. J. Int.*, 2013, 195, 159–175.
16 F. N. Skomurski, S. Kerisit and K. M. Rosso, *Geochim. Cosmochim. Acta*, 2010, 74, 4234–4248.
17 S. Nie, E. Starodub, M. Monti, D. A. Siegel, L. Vergara, G. F. El, N. C. Bartelt, l. F. J. de and K. F. McCarty, *J. Am. Chem. Soc.*, 2013, 135, 10091–10098.
18 C. Ratnasamy and J. P. Wagner, *Catal. Rev.*, 2009, 51, 325–440.
19 L. Giraldo, A. Erto and J. Moreno-Pirajań, *Adsorption*, 2013, 19, 465–474.
20 X. S. Wang, H. J. Lu, L. Zhu, F. Liu and J. J. Ren, *Adsorpt. Sci.Technol.*, 2010, 28, 407–417.
21 T. S. Pasakarnis, M. I. Boyanov, K. M. Kemner, B. Mishra, E. J. O'Loughlin, G. Parkin and M. M. Scherer, *Environ. Sci. Technol.*, 2013, 47, 6987–6994.
22 C. A. Gorski and M. M. Scherer, *Environ. Sci. Technol.*, 2009, 43, 3675–3680.
23 M. L. Peterson, G. E. Brown Jr, G. A. Parks and C. L. Stein, *Geochim. Cosmochim. Acta*, 1997, 61, 3399–3412.
24 K. Ravindra, R. Sokhi and R. Van Grieken, *Atmos. Environ.*, 2008, 42, 2895–2921.
25 D. Adamović, J. Dorić and M. Vojinović-Miloradov, *Causes, Impacts and Solutions to Global Warming*, Springer, 2013, pp. 333–342.
26 A. Richter, J. P. Burrows, H. Nüß, C. Granier and U. Niemeier, *Nature*, 2005, 437, 129–132.
27 D. Jordanova, N. Jordanova, P. Lanos, P. Petrov and T. Tsacheva, *Geochem., Geophys., Geosyst.*, 2012, 13, Q08Z49.
28 Q. Zhang, G. Sun, S. Fang, W. Tian, X. Li and H. Wang, *Sci.Total Environ.*, 2013, 450–451, 250–258.
29 D. L. Hartmann, A. M. G. Klein Tank, M. Rusticucci, L. V. Alexander, S. Brönnimann, Y. Charabi, F. J. Dentener, E. J. Dlugokencky, D. R. Easterling, A. Kaplan, B. J. Soden, P. W. Thorne, M. Wild and P. M. Zhai, in *Climate Change2013: The Physical Science Basis. Contribution of Working Group I to the Fifth Assessment Report of the Intergovernmental Panel on Climate Change*, ed. T. F. Stocker, D. Qin, G. - K. Plattner, M. Tignor, S. K. Allen, J. Boschung, A. Nauels, Y. Xia, V. Bex and P. M. Midgley, Cambridge University Press, Cambridge, United Kingdom and New York, NY, USA, 2013.
30 N. A. Eltouny and P. A. Ariya, *Ind. Eng. Chem. Res.*, 2012, 51,12787–12795.
31 F. Vereda, J. de Vicente and R. Hidalgo-Álvarez, *Langmuir*, 2007, 23, 3581–3589.
32 Thermo Fischer Scientific Inc., 2013.
33 V. Mani, in *Applications of Solid Phase Microextraction*,ed. J. Pawliszyn, The Royal Society of Chemistry, 1999, pp. 57–72.
34 J. Pawliszyn, *J. Chromatogr. Sci.*, 2000, 38, 270–278.
35 United Chemical Technologies., 2014.
36 Thermo Fischer Scientific Inc., 2013.
37 N. Eltouny, McGill, 2014.
38 IUPAC, in *The ''Gold Book''*, ed. A. D. McNaught and A. Wilkinson, Blackwell Scientific Publications, Oxford,2nd edn, 1997.
39 A. P. Grosvenor, B. A. Kobe and N. S. McIntyre, *Surf. Sci.*,2004, 565, 151–162.
40 S. Laurent, D. Forge, M. Port, A. Roch, C. Robic, L. VanderElst and R. N. Muller, *Chem. Rev.*, 2008, 108, 2064–2110.
41 A. Kalantzopoulos, S. Birbatakoy and F. Roubani-Kalantzopoulou, *Atmos. Environ.*, 1998, 32, 1811–1816.
42 I. Langmuir, *J. Am. Chem. Soc.*, 1918, 40, 1361–1403.
43 H. Freundlich, *Trans. Faraday Soc.*, 1932, 28, 195–201.
44 J. Toth, *Adv. Colloid Interface Sci.*, 1995, 55, 1–239.45 R. Sips, *J. Chem. Phys.*, 1950, 18, 1024–1026.
46 O. Redlich and D. L. Peterson, *J. Phys. Chem.*, 1959, 63, 1024.
47 W. Ranke and Y. Joseph, *Phys. Chem. Chem. Phys.*, 2002, 4,2483–2498.
48 OriginLab Corporation.
49 O. M. Akpa and E. I. Unuabonah, *Desalination*, 2011, 272,20–26.
50 C. M. Saffron, J.-H. Park, B. E. Dale and T. C. Voice, *Environ.Sci. Technol.*, 2006, 40, 7662–7667.

51 W. Rudzinski, S.-L. Lee, C.-C. S. Yan and T. Panczyk, *J. Phys.Chem. B*, 2001, 105, 10847–10856.
52 M. Bülow, M. Jaroniec and J. Piotrowska, *Thin Solid Films*, 1982, 88, 373–379.
53 C.-h. Yang, *J. Colloid Interface Sci.*, 1998, 208, 379–387.
54 M. A. Arocha, A. P. Jackman and B. J. McCoy, *Environ. Sci.Technol.*, 1996, 30, 1500–1507.
55 S. Agnihotri, M. J. Rood and M. Rostam-Abadi, *Carbon*,2005, 43, 2379–2388.
56 F. Mou, J. Guan, Z. Xiao, Z. Sun, W. Shi and X.-a. Fan, *J. Mater. Chem.*, 2011, 21, 5414–5421.
57 M. C. Biesinger, B. P. Payne, A. P. Grosvenor, L. W. M. Lau, A. R. Gerson and R. S. C. Smart, *Appl. Surf. Sci.*, 2011, 257,2717–2730.
58 G. B. D. Beamson, *High resolution XPS of organic polymers: the Scienta ESCA300 database*, Wiley, Chichester [England]; New York, 1992.
59 D. J. Miller, M. C. Biesinger and N. S. McIntyre, *Surf.Interface Anal.*, 2002, 33, 299–305.
60 K. Volgmann, F. Voigts and W. Maus-Friedrichs, *Surf. Sci.*,2012, 606, 858–864.
61 T. Kendelewicz, S. Kaya, J. T. Newberg, H. Bluhm,N. Mulakaluri, W. Moritz, M. Scheffler, A. Nilsson,R. Pentcheva and G. E. Brown, *J. Phys. Chem. C*, 2013, 117,2719–2733.
62 T. Kendelewicz, P. Liu, C. S. Doyle, G. E. Brown Jr, E. J. Nelson and S. A. Chambers, *Surf. Sci.*, 2000, 453, 32–46.
63 M. Keiluweit and M. Kleber, *Environ. Sci. Technol.*, 2009, 43,3421–3429.
64 H. Miura, R. Ansai and H. Kawai, *React. Kinet. Catal. Lett.*,1994, 53, 323–329.
65 H. Kuhlenbeck, S. Shaikhutdinov and H.-J. Freund, *Chem.Rev.*, 2013, 113, 3986–4034.
66 C. Kuhrs, Y. Arita, W. Weiss, W. Ranke and R. Schlogl, *Top.Catal.*, 2001, 14, 111–123.
67 F. Heinrich, C. Schmidt, E. Löffler, M. Menzel and W. Grünert, *J. Catal.*, 2002, 212, 157–172.
68 H. Liu, A. I. Kozlov, A. P. Kozlova, T. Shido and Y. Iwasawa, *Phys. Chem. Chem. Phys.*, 1999, 1, 2851–2860.
69 G. A. Waychunas and H. Zhang, *Elements*, 2008, 4, 381–387.
70 A. S. Madden and M. F. Hochella Jr, *Geochim. Cosmochim. Acta*, 2005, 69, 389–398.
71 N. Mulakaluri, R. Pentcheva, M. Wieland, W. Moritz and M. Scheffler, *Phys. Rev. Lett.*, 2009, 103, 176102.
72 J. H. P. S. N. Seinfeld, *Atmospheric chemistry and physics:from air pollution to climate change*, J. Wiley, Hoboken, N.J., 2006.
73 J. A. Rodriguez, T. Jirsak, G. Liu, J. Hrbek, J. Dvorak andA. Maiti, *J. Am. Chem. Soc.*, 2001, 123, 9597–9605.
74 J. Haubrich, R. G. Quiller, L. Benz, Z. Liu and C. M. Friend, *Langmuir*, 2010, 26, 2445–2451.
75 K. I. Hadjiivanov, D. G. Klissurski and V. P. Bushev, *J. Chem.Soc., Faraday Trans.*, 1995, 91, 149–153.
76 B. K. Min, R. G. Quiller, L. J. Deiner and C. M. Friend, *J. Phys. Chem. B*, 2005, 109, 20463–20468.
77 L. A. Wijenayaka, G. Rubasinghege, J. Baltrusaitis and V. H. Grassian, *J. Phys. Chem. C*, 2012, 116, 12566–12577.
78 D. E. Latta, C. A. Gorski, M. I. Boyanov, E. J. O'Loughlin, K. M. Kemner and M. M. Scherer, *Environ. Sci. Technol.*, 2012, 46, 778–786.
79 C. A. Gorski, J. T. Nurmi, P. G. Tratnyek, T. B. Hofstetter and M. M. Scherer, *Environ. Sci. Technol.*, 2009, 44, 55–60.
80 M. L. Peterson, A. F. White, G. E. Brown and G. A. Parks, *Environ. Sci. Technol.*, 1997, 31, 1573–1576.
81 K. H. Kim and J. S. Choi, *J. Phys. Chem.*, 1981, 85, 2447–2450.
82 S. Poulin, R. França, L. Moreau-Bélanger and E. Sacher, *J. Phys. Chem. C*, 2010, 114, 10711–10718.
83 P. Mills and J. L. Sullivan, *J. Phys. D: Appl. Phys.*, 1983, 16, 723.
84 A. G. B. Williams and M. M. Scherer, *Environ. Sci. Technol.*,2004, 38, 4782–4790.
85 T. B. Hofstetter, R. P. Schwarzenbach and S. B. Haderlein, *Environ. Sci. Technol.*, 2002, 37, 519–528.